Surface and bottom marine heatwave characteristics in the Barents Sea: a model study

Vidar S. Lien[1*], Roshin P. Raj[2], Sourav Chatterjee[3]

[1]Institute of Marine Research, Norway

[2]Nansen Environmental and Remote Sensing Center, Norway

[3]National Centre for Polar and Ocean Research, Ministry of Earth Sciences, India

[*]Correspondence to: Vidar S. Lien (vidar.lien@hi.no)

Abstract. Anomalously warm oceanic events, often termed marine heatwaves, can potentially impact the ecosystem in the affected region and has therefore become a hot topic for research in recent years. Determining the intensity and spatial extent of marine heatwaves, however, depends on the definition and climatological average used. Moreover, the stress applied by the heatwave to the marine ecosystem will depend on which component of the ecosystem is considered. Here, we utilize a model reanalysis (1991-2022) to explore the frequency, intensity, and duration of marine heatwaves in the Barents Sea, as well as regional heterogeneities. We find that major marine heatwaves are rather coherent throughout the region, but surface marine heatwaves occur more frequent while heatwaves on the ocean floor have longer duration. Moreover, we investigate the sensitivity to the choice of climatological average length when calculating marine heatwave statistics. Our results indicate that severe marine heatwaves may become more frequent in a future Barents Sea due to ongoing climate change.

1 Introduction

A marine heatwave (MHW) is a period of a warm spell in an ocean region and is usually defined as a period when the temperature exceeds a given threshold relative to a climatological average (e.g., Marbá et al., 2015; Hobday et al., 2016; Scannell et al., 2016; Hu et al., 2020; Huang et al., 2021). Due to the potential profound impact on marine life (e.g., Smale et al., 2019; Husson et al., 2022) and, hence, also socioeconomic impacts (Smith et al., 2021), MHWs have received increasing attention in recent years, see Oliver et al. (2021) for a comprehensive review of recent literature. While the criteria to define MHWs seem to converge to those proposed by Hobday et al. (2016), i.e., the temperature exceeding the 90th percentile of the moving climatological average, little attention has been given to the impact of the choice of climatological average on the MHW characteristics and statistics such as frequency, intensity and duration (Chiswell, 2022). The underlying trends of global ocean warming (e.g., Cheng et al., 2022) and regional climate variability (e.g., Smedsrud et al., 2022) both impact the MHW statistics, and some regions may eventually enter a state of permanent MHW, depending on the climatological average chosen. As an example, while Fröhlicher et al. (2018) found a doubling of MHW days between 1982 and 2016 globally, Chiswell

(2022) showed that accounting for climate change by removing the linear trend resulted in weaker MHWs in the tropics and stronger MHWs in the northern Pacific and Atlantic Oceans.

When MHWs are calculated as a timeseries for a whole region, possible regional heterogeneities may be masked, thereby reducing the applicability of using the timeseries as an MHW index. The Barents Sea is a complex shelf sea that mainly consists of a relatively warm and ice-free Atlantic Water dominated part in the south, and a cold, seasonally ice-covered Arctic Water dominated part in the north. The southern part is kept ice free by relatively warm and saline Atlantic Water entering to the southwest. The Atlantic Water gives up most of its heat (relative to the average temperature of the Polar Basin) to the atmosphere while en route (e.g., Gammelsrød et al., 2009; Smedsrud et al., 2013). Moreover, the inflow of Atlantic Water has been shown to be a precursor for interannual variability in the Barents Sea sea-ice cover (Onarheim et al., 2015; Schlichtholz, 2019) as well as the ocean heat content further downstream in the Barents Sea (Lien et al., 2017). Both the southern and northern Barents Sea have varying seasonal stratification, mainly from melting of sea ice in the north and solar insolation causing thermal stratification in the south (e.g., Smedsrud et al., 2013; Lind et al., 2018). The marine ecosystem is differing between the two main regions, with further diversification within each region. However, the extension of the two regimes is changing due to ongoing climate change, with the boreal, southern part expanding at the expense of the northern, Arctic part (e.g., Fossheim et al., 2015; Oziel et al., 2020). The Barents Sea is home to several important, commercial fish stocks, both pelagic (e.g., capelin (*Mallotus villosus*) and Norwegian spring spawning herring (*Clupea harengus*)) and demersal (e.g., northeast Arctic cod (*Gadus morhua*) and haddock (*Melanogrammus aeglefinus*)), in addition to a diverse marine ecosystem including large groups of marine mammals and sea birds as well as unique benthos communities (see Jakobsen and Ozhigin (2011) for a more comprehensive overview). Hence, MHWs may have profound impacts on marine living resources, but with different species exhibiting differences in resilience to MHW events (e.g., Husson et al., 2022). Recent studies on MHWs in the Barents Sea, however, have focused on the surface or the upper parts of the water column (Mohamed et al., 2022; Husson et al., 2022). Here, we investigate the occurrences of both surface and bottom MHWs in four contrasting environments in the Barents Sea. Moreover, we explore the differences in frequency, intensity and duration using varying climatological average lengths for estimating MHWs. We also focus on the highest-intensity MHW event in terms of cumulative degree-days and investigate its oceanic and atmospheric preconditioning and decline.

2 Data & Methods

2.1 Model data

We based our analysis on modelled daily averages from the EU Copernicus Marine Service ocean reanalysis for the Arctic region based on the TOPAZ model system for the period 1991-2022 (Sakov et al., 2012; Xie et al., 2016; Lien et al., 2016 product ref 1, Table 1), hereinafter termed *TOPAZ reanalysis*.

Table 1: Products used and their documentation.

Product ref. no.	Product ID & type	Data access	Documentation
1	ARCTIC_MULTIYEAR_PHY_002_003; Numerical models	EU Copernicus Marine Service Product (2022)	Quality Information Document (QUID): Xie & Bertino (2022) Product User Manual (PUM): Hackett et al. (2022)
2	Conductivity-Temperature-Depth data obtained in the Barents Sea	IMR database TINDOR (data accessible upon request)	
3	ERA5 Gridded Reanalysis (0.25 * 0.25 deg); monthly average on single level	EU Copernicus Climate Service Product (2023)	Hersbach et al., 2023

2.2 Ocean observation data

We have used available CTD (*Conductivity-Temperature-Depth*) casts (product ref. 2, Table 1), covering the period 1986 to 2020, for assessing the quality of the model dataset with regard to bottom temperatures in four regions of the Barents Sea (Fig. 1) before we use the models results to calculate MHW statistics. The CTD data were obtained from the Institute of Marine Research database TINDOR (The Integrated Database for Ocean Research).

2.3 Atmospheric data

Monthly averages of turbulent heatfluxes and outgoing longwave radiation for the period 1993 to 2021 were downloaded from the EU Copernicus Climate Service website (product ref. 3, Table 1).

2.4 Marine heatwave estimation method

We have adopted the definition of MHWs proposed by Hobday et al. (2016), where an MHW is defined as a period of more than five days where the temperature is above the 90^{th} percentile of the daily varying climatology averaged over a period of at least 30 years. Moreover, two consecutive events divided by a gap of two days or less is considered a single event.

The TOPAZ reanalysis covers the time period 1991-2022. In compliance with common standards by the World Meteorological Organization (WMO 2007; WMO 2015), we have chosen the period 1991-2020 as the climatological average period. To study the effect of changing the climatological average period, we have calculated the MHW statistics using also the 25-year period 1996-2020 and the 20-year period 2001-2020 as the climatological average periods.

We have chosen four sub-regions where we compute the daily spatially averaged surface and bottom temperatures representing contrasting marine environments: the Bear Island Trough in the south-western Atlantic Water inflow area to the Barents Sea; the adjacent Spitsbergen Bank which represents a productive, shallow bank with an Arctic marine environment; the Northeast Basin in the north-eastern Barents Sea which represents the outflow region where strongly modified Atlantic-derived water masses leave the Barents Sea; the Pechora Sea to the south-east which represents a shallow and coastal water influenced area (see map, Fig. 1). Our Bear Island Trough region is pushed towards the southern slope of the trough to cover the area around 72°30'N which is where the core of the main inflow branch carrying Atlantic Water to the Barents Sea is located (e.g., Skagseth et al., 2008).

For estimating MHW statistics we have used the python package provided by Eric C. J. Oliver: https://github.com/ecjoliver/marineHeatWaves and using the default settings.

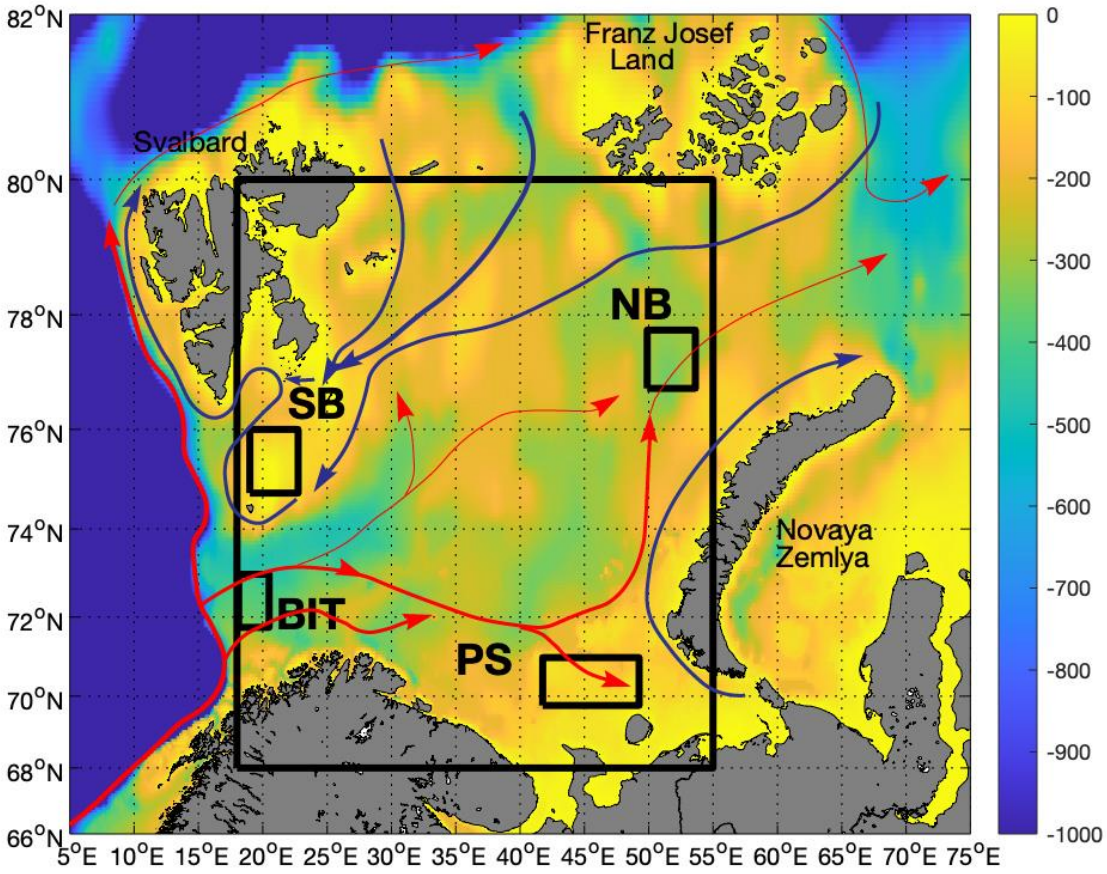

Figure 1:Update regions! Map of the Barents Sea. Colors show the bathymetry (in meters). Arrows show the main current patterns for Atlantic Water (red) and Arctic Water (blue). Boxes show regions for estimating marine heatwaves statistics from the TOPAZ reanalysis (black) and ROMS regional hindcast (blue). BIT: Bear Island Trough; NB: Northeast Basin; SB: Spitsbergen Bank; PS: Pechora Sea.

2.4 Model evaluation

The model product used in this study has previously been evaluated against a suite of ocean observations (e.g., Lien et al. (2016); Xie et al. (2019, 2023)). However, because we also used the model for analysis of MHWs near the ocean floor, we here provide an assessment of the quality of the model by direct comparison with observations of near-bottom temperature from CTD casts where available in the four sub-regions. The motivation for comparing only bottom temperatures is that

satellite sea surface temperature observations are assimilated into the TOPAZ reanalysis. Moreover, the sea surface temperature is also constrained by ocean-atmosphere bulk fluxes.

In this model quality assessment, we compared modelled and observed near-bottom temperatures averaged in time (monthly) and space (see sub-regions, Fig. 1). The modelled seasonal signal was removed from both model and observation timeseries before the correlation was calculated. The comparison is summarized in Table 2 and Supplementary Figure S1.

Table 2: Statistics summarizing the comparison between the models and observations at *N* CTD locations. Correlations are shown in boldface when $p < 0.05$ and underlined boldface when $p < 0.01$. BIT: Bear Island Trough; SB: Spitsbergen Bank; PS: Pechora Sea; NB: Northeast Basin.

Model	Statistic	BIT	SB	PS	NB
TOPAZ	*N*	202	49	34	11
	Bias [℃]	1.9	-2.1	-0.8	-0.6
	RMSd [℃]	2.0	2.4	1.0	0.7
	Correlation [*r*]	**0.55**	**0.39**	**0.78**	**0.66**

3 Results

We first calculated the MHW statistics based on the TOPAZ reanalysis for the full Barents Sea region for the period 1991-2022 (see Fig. 1 for area definition), which are summarized in figure 2 and Tables 3-5. A total of 29 MHWs were identified at the surface compared to 5 MHWs near the bottom, equating to a frequency of 0.90 year^{-1} at the surface and 0.16 year^{-1} near the bottom. The average maximum intensity was 1.41 ℃ and 1.07 ℃ at the surface and near the bottom, respectively. The duration was, on average, longer near the bottom (214 days) than at the surface (33 days). Moreover, we found a positive, decadal trend in the MHW frequency at the surface of 0.82 year^{-1} ($p < 0.05$), while for all the other metrics mentioned above, the decadal trends were non-significant.

Two periods are distinguished in terms of MHW cumulative intensity (℃ days), both at the surface and near the bottom. The strongest MHW in the Barents Sea as a whole, in terms of cumulative intensity, occurred in 2016 both at the surface and near the bottom (Fig. 3a,f). At the surface, the 2016 MHW had an average intensity of 1.29 ℃ (maximum of 3.41 ℃) and a total duration of 480 days (from December 19, 2015, to April 11, 2017). Near the bottom, the 2016 MHW had an average intensity of 1.10 ℃ (maximum of 1.28 ℃) and a total duration of 479 days (February 28, 2016, to June 20, 2017). The second strongest

MHW in terms of cumulative intensity in the Barents Sea as a whole, occurred in 2013 at the surface and in 2012 near the bottom (see Supplementary Figure S2). While an investigation on possible mechanisms for the decoupling between the surface and the bottom is beyond the scope of this work, we note that the 2012/13 MHW event was preceded by an extraordinarily large temperature anomaly but close to average volume transport in the Atlantic Water entering the Barents Sea to the southwest (e.g., ICES, 2022), as opposed to extraordinarily large volume transports preceding the 2016 MHW event (see below for more details). Moreover, previous studies have suggested that temperature anomalies that are advected into the Barents Sea at depth during the stratified summer season, can reemerge at the surface further downstream through vertical mixing during the following winter (e.g., Schlichtholz, 2019).

(a)

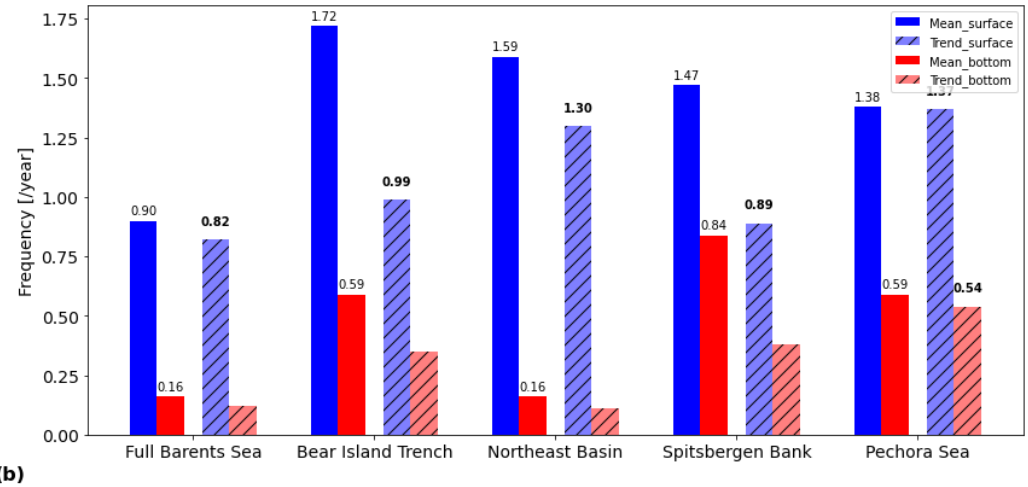
Mean_surface
Trend_surface
Mean_bottom
Trend_bottom
Frequency [/year]
1.75
1.50
1.25
1.00
0.75
0.50
0.25
0.00
0.90
0.82
1.72
0.59
0.99
1.59
0.16
1.30
1.47
0.84
0.89
1.38
0.59
0.54
Full Barents Sea
Bear Island Trench
Northeast Basin
Spitsbergen Bank
Pechora Sea

(b)

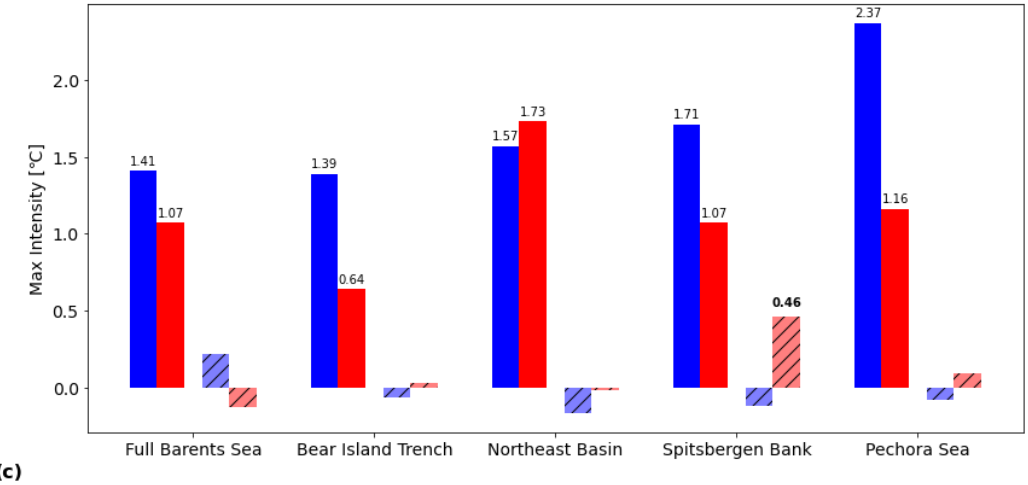
Max Intensity [°C]
2.0
1.5
1.0
0.5
0.0
1.41
1.07
1.39
0.64
1.57
1.73
1.71
1.07
0.46
2.37
1.16
Full Barents Sea
Bear Island Trench
Northeast Basin
Spitsbergen Bank
Pechora Sea

(c)

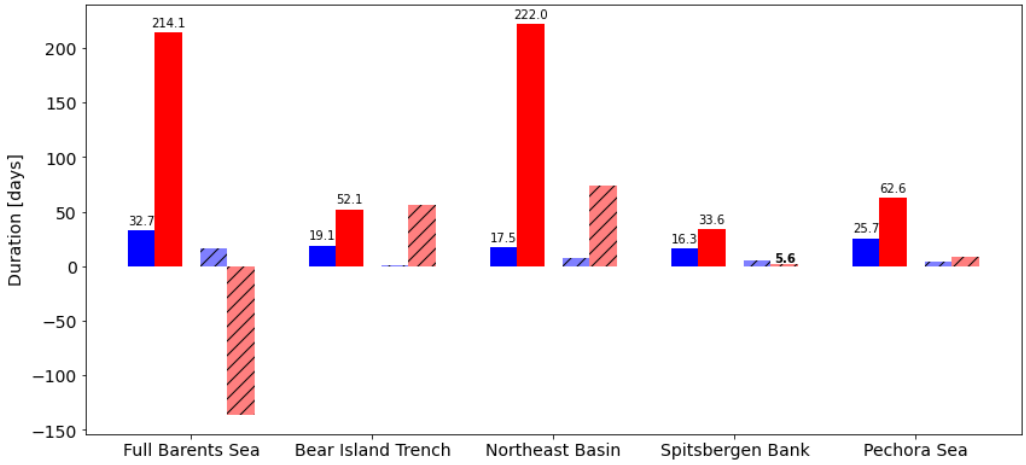
Duration [days]
200
150
100
50
0
−50
−100
−150
32.7
214.1
19.1
52.1
17.5
222.0
16.3
33.6
5.6
25.7
62.6
Full Barents Sea
Bear Island Trench
Northeast Basin
Spitsbergen Bank
Pechora Sea

134

Figure 2: Marine heatwave statistics for the full Barents Sea for the period 1991-2022, using 1991-2020 as the climate average period. a) Number of marine heatwave events per year; b) maximum intensity of the heatwave events; c) average marine heatwave duration. The associated decadal trends are shown in hatched colors. The trend is provided in boldface if significant to 95% ($p < 0.05$). Surface values are shown by blue bars and bottom values are shown by red bars. Based on data from the TOPAZ reanalysis.

To investigate possible regional heterogeneity in MHWs within the Barents Sea, we calculated MHW statistics in the four sub-regions depicted in figure 1. The results are summarized in Table 3, 4, and 5. In all regions, we found a higher frequency of MHW events than for the Barents Sea as a whole (except for near the bottom in the Northeast Basin). Moreover, all regions showed a larger, positive decadal trend in the frequency compared with the Barents Sea as a whole, although near the bottom only the trend in the Pechora Sea was found to be statistically significant ($p < 0.05$; Table 3). For the average maximum intensity, at the surface, we found that the Bear Island Trough, which is the upstream inflow region, had similar statistics as for the Barents Sea as a whole, while for the other three regions the intensity was generally larger (Table 4). Near the bottom, the intensity in the Bear Island Trough was less than that of the Barents Sea as a whole, while in the downstream Northeast Basin the intensity was larger on average. In the two other regions the differences were smaller. In terms of duration, all the regions experienced shorter MWHs on average compared to the Barents Sea as a whole, and especially so near the bottom. The exception was the Northeast Basin, where the average duration of near-bottom MHWs was found to be comparable to that of the Barents Sea as a whole (Table 5).

To investigate further regional heterogeneity, we considered the MHW event in 2016 in each of the regions. At the surface, the 2016 MHW event was the most severe MHW event in terms of cumulative intensity in three out of the four sub-regions investigated. The exception was the Bear Island Trough, where the 2012 MHW event was more severe (not shown). Near the bottom, the 2016 MHW event was the most severe MHW event in all four regions (Fig. 3). The progression of the 2016 MHW event was comparable in all regions, except for the Spitsbergen Bank where the onset of the MHW occurred later, near mid-summer, compared to the other regions where the onset occurred during late winter. However, on the Spitsbergen Bank the 2016 MHW was preceded by several but less intense and intermittent MHWs. It is also worth noting that the onset in the other three regions, as well as the Barents Sea as a whole, occurred in late February/early March, except for in the upstream Bear Island Trough where the onset occurred in the beginning of April. Moreover, both the average and maximum MHW intensity was less in the Bear Island Trough compared to the other regions.

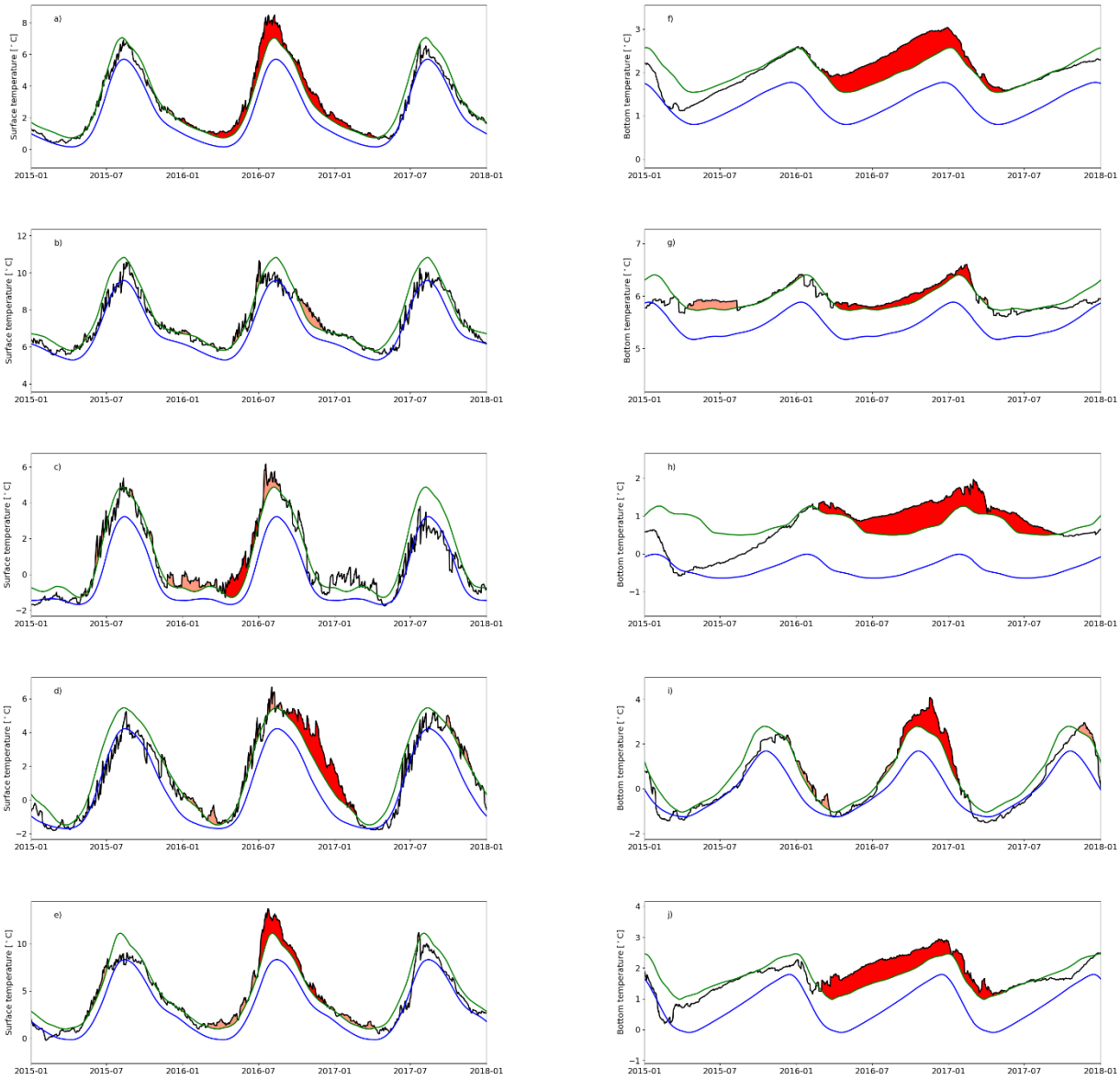

Figure 3: Time series (2015-2017; black lines) showing the temperature at the surface (left column) and near the bottom (right column) spatially averaged over the Barents Sea. Blue lines show daily climatology. Green lines show the 90th percentile. The highest intensity marine heatwave in terms of cumulative degree days for the full 1991-2022 period is shown in dark red shading. Other marine heatwaves are shown in pink shading. a) the full Barents Sea, surface; b) the Bear Island Trough, surface; c) the Northeast Basin, surface; d) the Spitsbergen Bank, surface; e) the Pechora Sea, surface; f) the full Barents Sea, bottom; g) the Bear Island Trough, bottom; h) the Northeast Basin, bottom; i) the

Spitsbergen Bank, bottom; j) the Pechora Sea, bottom. All panels show the period January 1st 2015 to January 1st 2018. Note the different scales on the y-axes.

3.1 Preconditioning and atmospheric forcing of 2016 MHW event

Leading up to the onset of the 2016 MHW, the inflow of warm Atlantic Water to the Barents Sea was above average during the whole of 2015 (ICES, 2022). However, during the following winter of 2015/16, the turbulent (latent and sensible) heat loss was between 20 and 70 Wm^{-2} below the 1993-2021 average in the southern Barents Sea (25-45E; 71-75N; i.e., along the Atlantic Water pathway through the Barents Sea; Fig. 4a), which was the lowest for the period 1993-2021. The reduced heat loss to the atmosphere occurred despite the preceding increase in advected oceanic heat (Fig. 4a,e). Note, that during the winter months, the solar radiation can be neglected due to the Polar Night conditions in the Barents Sea region. Moreover, wind-driven mixing during winter breaks down the upper water column stratification, connecting the surface with the deeper layers. Thus, the 2016 MHW event was preceded by an increased Atlantic Water heat transport and reduced heat loss to the atmosphere. While we did not perform a closed heat budget calculation, we note that the oceanic heat carried by the downstream outflow from the Barents Sea has previously been reported to be smaller than the inflow by an order of magnitude (e.g., Gammelsrød et al., 2009; Smedsrud et al., 2013), and that a previous study found that increased oceanic heat advection to the Barents Sea lead to increased ocean heat content in the interior Barents Sea (Lien et al., 2017).

In the following winter of 2016/17, i.e., during the decline of the 2016 MHW event, the turbulent heat loss and outgoing longwave radiation in the northern Barents Sea (25:45E; 76-80N; Fig. 4b,e,f) reached the largest values in the 1993-2021 period. This was likely enhanced by a record low winter sea ice extent (ICES, 2022) and negative cloud cover anomaly in the northern Barents Sea (not shown). In the southern Barents Sea, however, no heat loss anomaly at the ocean surface was observed during the winter 2016/17 (Fig. 4b), but the Atlantic Water transport through the Barents Sea Opening decreased during 2016 (ICES, 2022). Thus, the 2016 MHW event in the Barents Sea can be linked to the combined effect of increased Atlantic water transport into the Barents Sea, as well as reduced oceanic heat loss in the southern Barents Sea during the onset and increased oceanic heat loss in the northern Barents Sea during the decline.

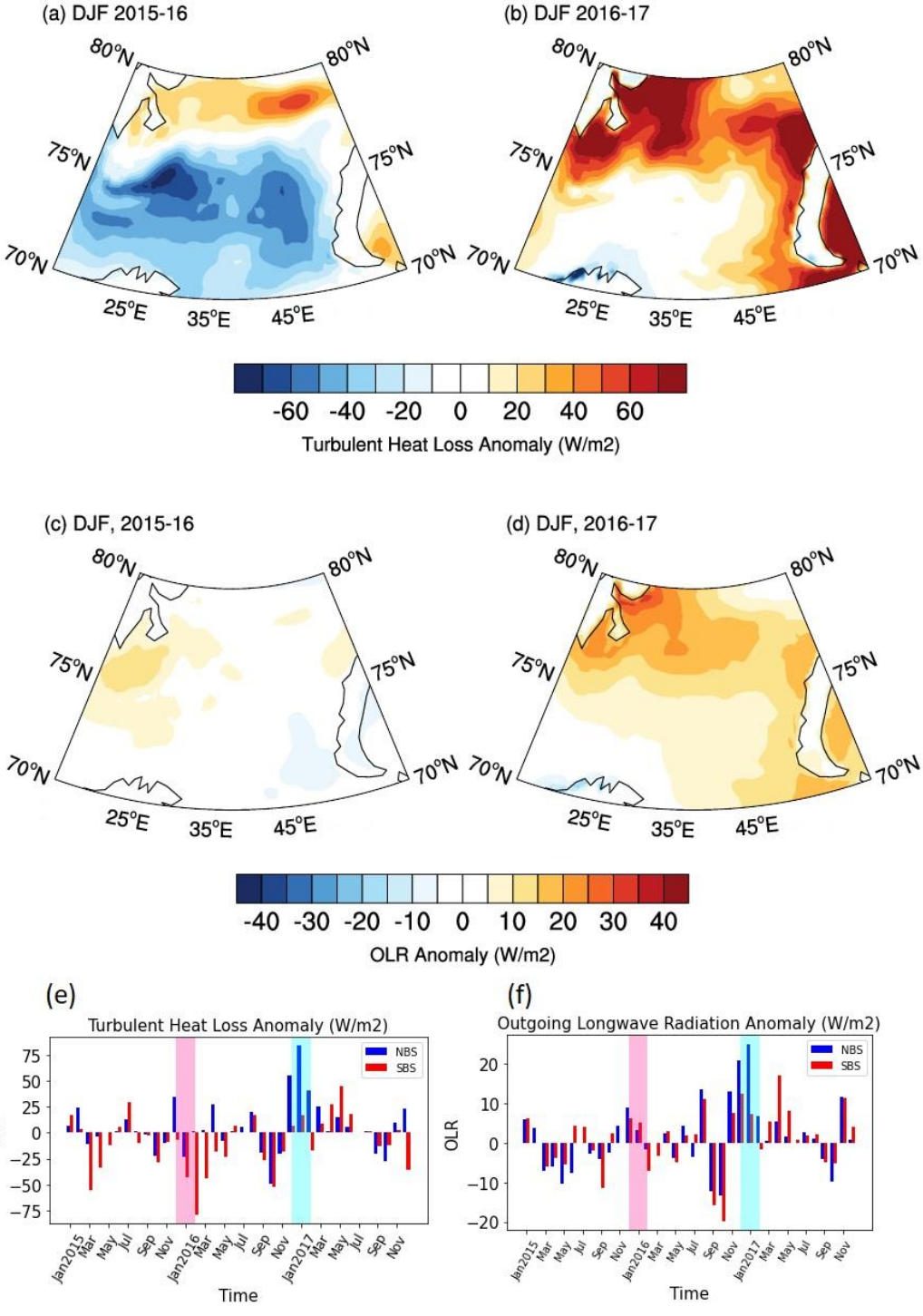
(a) DJF 2015-16
(b) DJF 2016-17
80°N
75°N
70°N
25°E
35°E
45°E
-60 -40 -20 0 20 40 60
Turbulent Heat Loss Anomaly (W/m2)
(c) DJF, 2015-16
(d) DJF, 2016-17
-40 -30 -20 -10 0 10 20 30 40
OLR Anomaly (W/m2)
(e)
Turbulent Heat Loss Anomaly (W/m2)
THL
NBS
SBS
Time
(f)
Outgoing Longwave Radiation Anomaly (W/m2)
OLR
Jan2015
Mar
May
Jul
Sep
Nov
Jan2016
Jan2017

193

Figure 4: Atmospheric preconditioning leading up to the MHW depicted in Fig. 3. (a,b) DJF (December(-1), January, February (0)) turbulent (latent + sensible) heat loss anomaly (W/m2) for 2016 (a) and 2017 (b). Same as (a,b) but for Outgoing Longwave Radiation (OLR). Positive values indicate upward fluxes. Monthly mean turbulent heat loss (e) and OLR (f) over northern (blue, 25:45E; 76-80N) and southern (red, 25-45E; 71-75N) Barents Sea. The onset (DJF, 2015-16) and decay (DJF, 2016-17) phase of the 2016 MHW event are shaded in pink and cyan colours. Data: ERA5

3.2 Effect of changing baselines

Next, we investigated the effect of changing the climatological average period from 30 years (1991-2020) to 25 years (1996-2020) and 20 years (2001-2020) when calculating the MHW statistics for both the surface and the bottom (Tables 3-5).

For all regions, including the Barents Sea as a whole, we found that the frequency of surface MHWs decreased with decreasing length of the climatological average period. For near-bottom MHWs, the results were less clear except for a decrease in frequency in the two shallow bank regions (the Spitsbergen Bank and the Pechora Sea). Similarly, for the intensity at the surface, there was a general trend of decreasing average intensity with decreasing length of the climatological average period. There was also a trend of decreasing intensities near the bottom, except for in the two shallow bank regions. As opposed to the average frequency and intensity, the average duration seemed less dependent on the length of the climatological average period. Near the bottom, however, the duration was sensitive to the climatological average period length due to the low number of MHWs and the dominance of the 2012 and 2016 MHW events.

Table 3: Average frequency of marine heatwaves +/- the decadal trend for two different baseline periods, 1961-1990 and 1991-2020. The baseline period 1991-2020 is also used for the detrended, full time series (1961-2020). The trend is provided in boldface if significant to 95% ($p < 0.05$), or in italics if not significant ($p > 0.05$). Values for the surface are shown on top and values for bottom are shown below. BIT: Bear Island Trough; SB: Spitsbergen Bank; PS: Pechora Sea; NB: Northeast Basin.

Baseline \ Area	**FULL**	**BIT**	**SB**	**PS**	**NB**
1991 - 2020	**0.90 + 0.82** **0.16** + *0.12*	**1.72** + **0.99** **0.59** + *0.35*	**1.47** + **0.89** **0.84** + *0.38*	**1.38** + **1.37** **0.59** + **0.54**	**1.59** + **1.30** **0.16** + *0.11*
1996 - 2020	**0.84 + 0.85** **0.44** + *0.18*	**1.53 + 0.90** **0.59** + *0.39*	**1.16** + *0.78* **0.81** + *0.44*	**1.09 + 1.10** **0.53 + 0.47**	**1.44 + 1.36** **0.31** + *0.21*
2001 – 2020	**0.59 + 0.66** **0.19** + *0.14*	**1.19 + 0.64** **0.53** + *0.37*	**1.09 + 0.82** **0.59** + *0.35*	**0.84 + 0.89** **0.25 + 0.23**	**1.28 + 1.22** **0.25** + *0.24*

Table 4: Same as Table 3 but showing average maximum intensity (in °C).

Reference period \ Area	FULL	BIT	SB	PS	NB
1991 - 2020	**1.41** + *0.22* **1.07** – *0.13*	**1.39** - *0.07* **0.64** + *0.03*	**1.71** - *0.12* **1.07** + **0.46**	**2.37** + *0.08* **1.16** + *0.09*	**1.57** - *0.17* **1.73** - *0.02*
1996 - 2020	**1.35** + *0.23* **0.96** + *0.17*	**1.35** - *0.05* **0.61** - *0.01*	**1.57** - *0.07* **1.17** + **0.58**	**2.22** + *0.49* **1.16** + *0.03*	**1.58** - *0.25* **1.48** + *0.06*
2001 - 2020	**1.26** + *0.32* **0.85** + *0.06*	**1.31** – *0.08* **0.51** + *0.00*	**1.49** – *0.13* **1.17** + **0.51**	**2.01** + *0.35* **1.15** – *0.10*	**1.49** – *0.29* **1.43** – *0.01*

Table 5: Same as Table 3 but showing average duration (in days).

Baseline \ Area	FULL	BIT	SB	PS	NB
1991 - 2020	**32.7** + *16.2* **214.1** – *135.8*	**19.1** + *1.3* **52.1** + *56.2*	**16.3** + **5.6** **33.6** + *1.5*	**25.7** + *4.5* **62.6** + *8.7*	**17.5** + *7.8* **222.0** + *74.4*
1996 - 2020	**39.5** + *16.2* **139.2** + *32.0*	**20.0** - *0.6* **37.8** + *29.8*	**16.5** + *4.5* **28.7** - *3.5*	**70.8** + *24.0* **55.1** + *3.1*	**17.0** + *3.7* **109.9** - *36.3*
2001 - 2020	**38.0** – *13.9* **136.4** – *2.1*	**19.8** – *1.0* **37.8** + *24.0*	**15.6** – *0.07* **36.6** – *8.4*	**20.8** + *1.7* **101.6** + *0.7*	**15.3** + **6.8** **122.4** – *41.1*

4 Discussion

We have estimated average MHW frequency, duration, and intensity at the surface and near the bottom in the Barents Sea, based on an ocean reanalysis for the period 1991-2022. Moreover, we have investigated the impact of changing climatological average period length when estimating MHW statistics in the Barents Sea. We found two dominating and pervasive MHW events in the Barents Sea in the last 30 years that affected the whole region.

Previous studies of MHWs, including in the Barents Sea, have mainly focused on the ocean surface due to the availability of satellite remote sensing sea surface temperature data (e.g., Mohamed et al., 2022). Our results identified significant MHW events also near the ocean bottom in the Barents Sea, and that bottom MHWs tend to have lower frequency and intensity but longer duration compared to surface MHWs. Note, however, that these statistics need to be interpreted with care, especially the statistics on near-bottom MHWs due to the low number of events (5 near-bottom MHWs were detected in the Barents Sea during 1991-2022). Among other things, this severely affected the statistical significance of the trend estimates. Nevertheless, the longer duration near the bottom was more pronounced in the eastern parts of the Barents Sea, as represented by the Pechora

Sea and the Northeast Basin. One likely explanation is the strong reduction in sea-ice formation in the shallow Pechora Sea in the south-eastern Barents Sea and on the Novaya Zemlya Bank adjacent to the Northeast Basin, and thus a reduction in the formation of cold, brine-enriched water. The eastern Barents Sea is one of the regions that has experienced the largest changes in the sea-ice cover in recent decades (e.g., Yang et al., 2016; Onarheim and Årthun, 2017) and has thus experienced a strong reduction in the formation of cold, brine-enriched bottom water. Midttun (1985) observed very cold and saline water in the deeper parts of the Northeast Basin following cold winters in the 1970s, while Lien & Trofimov (2013) reported no such bottom water following the warmer winter of 2007/08. Occasional presence of such cold bottom water further west in the Barents Sea, adjacent to the Bear Island Trough, has been hypothesized to cause differences in the position of the Polar Front at the bottom, as detected by bottom living organisms, compared to higher in the water column based on hydrographic properties in the pelagic zone (Jørgensen et al., 2015). Thus, the transition indicated by bottom MHWs in the eastern Barents Sea may have a profound impact on bottom fauna by allowing boreal species with less resilience to below-zero temperatures to settle.

Previous findings by Mohamed et al (2022), based on satellite remote sensing sea-surface temperature data, contrasted the Spitsbergen Bank area showing no trend in MHW frequency and duration with the Pechora Sea area showing significant trends in both frequency and duration. None of the two regions showed significant trends in MHW intensity. Our findings agree with those of Mohamed et al. (2022) that the Pechora Sea has experienced a positive trend in MHW frequency and not in intensity, but our results showed no significant trend in duration, at the surface. Our results indicated that there is also a significant, positive trend in MHW frequency near the bottom in the Pechora Sea (but not in intensity and duration). Moreover, our results showed positive trends in both the MHW frequency and duration on the Spitsbergen Bank (at the surface), although we did not find a statistically significant trend in MHW intensity. But our results indicated a positive trend in the MHW intensity near the bottom on the Spitsbergen Bank. Note, however, that the Spitsbergen Bank is also the area where the TOPAZ reanalysis showed the largest bias and RMS deviation, as well as the lowest correlation, when compared with in-situ temperature observations. Thus, we cannot draw firm conclusions whether our results for the Spitsbergen Bank area contradict the findings of Mohamed et al. (2022).

Our findings that the strong 2016 MHW event was preceded by stronger than average Atlantic Water inflow and anomalously weaker ocean-to-atmosphere heat loss further suggest that MHWs may become more frequent and severe in terms of intensity and duration in a future Barents Sea with continued increase in oceanic heat advection from the North Atlantic (e.g., Årthun et al., 2019) in combination with reduced ocean-to-atmosphere heat loss within the Barents Sea (e.g., Skagseth et al., 2020).

5 Data availability

A list of the data products utilized in this paper, along with their availability and links to their documentation, is provided in Table 1.

6 Author contribution

All authors contributed to the design, analysis, and writing of the paper.

7 Competing interests

The authors declare that they have no conflict of interest.

8 Acknowledgements

This work was funded by the Copernicus Marine Service, contract #21002L1-COP-MFC ARC-5100.

9 References

Årthun, M., Eldevik, T., and Smedsrud, L. H.: The role of Atlantic heat transport in future Arctic winter sea ice loss. J Clim., 32, 3327-3341, 2019

Cheng, L., von Schuckmann, K., Abraham, J. P., Trenberth, K. E., Mann, M. E., Zanna, L., England, M. H., Zika, J. D., Fasullo, J. T., Yu, Y., Pan, Y., Zhu, J., Newsom, E. R., Bronselaer, B., and Lin X.: Past and future ocean warming. Nat Rev Earth Environ., 3, 776-794, 2022

Chiswell, S. M.: Global Trends in Marine Heatwaves and Cold Spells: The Impacts of Fixed Versus Changing Baselines. J Geophys Res Oceans, 127, e2022JC018757, 2022

EU Copernicus Marine Service Product: Arctic Ocean Physics Reanalysis, Mercator Ocean International [dataset], https://doi.org/10.48670/moi-00007, 2022.

EU Copernicus Climate Service Product: ERA5 monthly averaged data on single levels from 1940 to present [dataset], https://doi.org/10.24381/cds.f17050d7, 2023.

Fossheim, M., Primicerio, R., Johannesen, E., Ingvaldsen, R. B., Aschan, M. M. and Dolgov, A. V.: Recent warming leads to a rapid borealization of fish communities in the Arctic. Nat Clim Change, doi: 10.1038/nclimate2647, 2015

Frölicher, T. L., Fischer, E. M. and Gruber, N.: Marine heatwaves under global warming. Nature, 560(7718), 360–364. https://doi.org/10.1038/s41586-018-0383-9, 2018

Gammelsrød, T., Leikvin, Ø., Lien, V., Budgell, W. P., Loeng, H., and Maslowski. W.: Mass and Heat transports in the NE Barents Sea: Observations and Models. J. Mar. Sys., 75**,** 56-69, doi: 10.1016/j.jmarsys.2008.07.010, 2009

Hackett, B., Bertino, L., Alfatih, A., Burud, A., Williams, T., Xie, J., Yumruktepe, C., Wakamatsu, T., and Melsom, A.: EU Copernicus Marine Service Product User Manual for the Arctic Ocean Physics Reanalysis Product, ARCTIC_MULTIYEAR_PHY_002_003, Issue 5.15, Mercator Ocean International,

https://catalogue.marine.copernicus.eu/documents/PUM/CMEMS-ARC-PUM-002-ALL.pdf, last access: 20 June, 2023, 2022

Hersbach, H., Bell, B., Berrisford, P., Biavati, G., Horányi, A., Muñoz Sabater, J., Nicolas, J., Peubey, C., Radu, R., Rozum, I., Schepers, D., Simmons, A., Soci, C., Dee, D., and Thépaut, J-N.: ERA5 hourly data on single levels from 1940 to present. Copernicus Climate Change Service (C3S) Climate Data Store (CDS), DOI: 10.24381/cds.adbb2d47 (Accessed on 08-09-2022), 2023

Hobday, A. J., Alexander, L. V., Perkins, S. E., Smale, D. A., Straub, S. C., Oliver, E. C. J., Benthuysen, J. A., Burrows, M. T., Donat, M. G., Feng, M., Holbrook, N. J., Moore, P. J., Scannell, H. A., Gupta, A. S., Wernberg, T.: A hierarchical approach to defining marine heatwaves. Progr. Oceanogr., 141, 227-238, 2016

Hu, S., Zhang, L., Qian, S.: Marine heatwaves in the Arctic region: Variation in different ice covers. Geophysical Research Letters, 47, e2020GL089329. https://doi.org/10.1029/2020GL089329, 2020

Huang, B., Wang, Z., Yin, X., Arguez, A., Graham, G., Liu, C., Smith, T., Zhang H.-M.: Prolonged Marine Heatwaves in the Arctic: 1982-2020. Geophys. Res. Lett., 48, e2021GL095590, https://doi.org/10.1029/2021GL095590, 2021

Husson, B., Lind, S., Fossheim, M., Kato-Solvag, H., Skern-Mauritzen, M., Pécuchet, L., Ingvaldsen, R. B., Dolgov, A. V. and Primicerio, R.: Successive extreme climatic events lead to immediate, large-scale, and diverse responses from fish in the Arctic. Global Change Biol, 28, 3728-3744, 2022

ICES: Working Group on the Integrated Assessments of the Barents Sea (WGIBAR). ICES Scientific Reports, 4:50, 235 pp. http://doi.org/10.17895/ices.pub.20051438, 2022

Jakobsen, T., and Ozhigin, V. K., [Eds.]: The Barents Sea - Ecosystem, Resources, Management: Half a century of Russian-Norwegian cooperation. 825 pp, Tapir Academic Press, Trondheim, Norway, 2011

Jørgensen, L. L., Ljubin, P., Skjoldal, H. R., Ingvaldsen, R. B., Anisimova, N. and Manushin, I.: Distribution of benthic megafauna in the Barents Sea: baseline for an ecosystem approach to management. ICES J Mar Sci., 72(2), 595-613, doi:10.1093/icesjms/fsu106, 2015

Lien, V. S. and Trofimov, A. G.: Formation of Barents Sea Branch Water in the north-eastern Barents Sea. Polar Res, 32, 18905, 2013

Lien, V. S., Hjøllo, S. S., Skogen, M. D., Svendsen, E., Wehde, H., Bertino, L., Counillon, F., Chevallier, M. and Garric, G.: An assessment of the added value from data assimilation on modelled Nordic Seas hydrography and ocean transports. Ocean Modell., 99, 43-59. doi: 10.1016/j.ocemod.2015.12.010, 2016

Lien, V. S., Schlichtholz, P., Skagseth, Ø., and Vikebø, F.B.: Wind-driven Atlantic water flow as a direct mode for reduced Barents Sea ice cover. J. Climate, 30, 803-812, 2017

Lind, S., Ingvaldsen, R. B. and Furevik, T.: Arctic warming hotspot in the northern Barents Sea linked to declining sea-ice import. Nat Clim Change, 8, 634-639, 2018

Marbà, N., Jordà, G., Agustí, S., Girard, C. and Duarte, C. M.: Footprints of climate change on Mediterranean Sea biota. Front Mar Sci., 2. https://doi.org/10.3389/fmars.2015.00056, 2015

Midttun, L.: Formation of dense bottom water in the Barents Sea. Deep-Sea Res Part A, 32, 1233-1241, 1985

Mohamed, B., Nilsen, F. and Skogseth, R.: Marine Heatwaves Characteristics in the Barents Sea Based on High Resolution Satellite Data (1982-2020). Front Mar Sci., 9, 821646, doi:10.3389/fmars.2022.821646, 2022

Oliver, E. C. J., Benthuysen, J. A., Darmaraki, S., Donat, M. G., Hobday, A. J., Holbrook, N. J., et al.: Marine heatwaves. Annual Review of Marine Science, 13(1), 313–342. https://doi.org/10.1146/annurev-marine-032720-095144, 2021

Onarheim, I. H., Eldevik, T., Årthun, M., Ingvaldsen, R. B., and Smedsrud, L. H.: Skillful prediction of Barents Sea ice cover. *Geophys. Res. Lett.,* 42(13), 5364-5371, 2015

Onarheim, I. H., and Årthun, M.: Toward an ice-free Barents Sea. Geophys. Res. Lett., 44, 8387–8395, doi:10.1002/2017GL074304, 2017

Oziel, L., Baudena, A., Ardyna, M., Massicotte, P., Randelhoff, A., Sallee, J.-B., Ingvaldsen, R. B., Devred, E., and Babin, M.: Faster Atlantic currents drive poleward expansion of temperate phytoplankton in the Arctic Ocean. Nat Commun., 11(1), 1705, doi:10.1038/s41467-020-15485-5, 2020

Sakov, P., Counillon, F., Bertino, L., Lisæter, K. A., Oke, P. R., and Korablev, A.: TOPAZ4: an ocean-sea ice data assimilation system for the North Atlantic and Arctic. Ocean Sci., 8(4), 633-656, 2012

Scannell, H. A., Pershing, A. J., Alexander, M. A., Thomas, A. C. and Mills, K. E.: Frequency of marine heatwaves in the north Atlantic and north Pacific since 1950. Geophys Res Lett., 43(5), 2069–2076. https://doi.org/10.1002/2015GL067308, 2016

Schlichtholz, P.: Subsurface ocean flywheel of coupled climate variability in the Barents Sea hotspot of global warming. Sci. Reports, 9, 13692. https://doi.org/10.1038/s41598-019-49965-6, 2019

Skagseth, Ø., *et al.*: Volume and Heat Transports to the Arctic Ocean via the Norwegian and Barents Seas. In: *Arctic Subarctic ocean fluxes: Defining the Role of the Northern Seas in Climate*, Dickson R, Meincke J, Rhines P (Eds.), pp. 45-64, Springer, New York, 2008

Skagseth, Ø., Eldevik, T., Årthun, M., Asbjørnsen, H., Lien, V. S., and Smedsrud, L. H.: Reduced efficiency of the Barents Sea cooling machine. Nat Clim Change, doi.org/10.1038/s41558-020-0772-6, 2020

Smale, D. A., Wernberg, T., Oliver, E. C. J., Thomsen, M., Harvey, B. P., Straub, S. C., et al.: Marine heatwaves threaten global biodiversity and the provision of ecosystem services. Nature Clim Change, 9(4), 306–312. https://doi.org/10.1038/s41558-019-0412-1, 2019

Smedsrud, L.H., Esau, I., Ingvaldsen, R.B., Eldevik, T., Haugan, P.M., Li, C., Lien, V.S., Olsen, A., Omar, A.M., Otterå, O.H., Risebrobakken, B., Sandø, A.B., Semenov, V.A. and Sorokina, S.A.: The role of the Barents Sea in the climate system. Rev Geophys., 51, 415-449, 2013

Smedsrud, L. H., Muilwijk, M., Brakstad, A., Madonna, E., Lauvset, S. K., Spensberger, C., Born, A., Eldevik, T., Drange, H., Jeansson, E., Li, C., Olsen, A., Skagseth, Ø., Slater, D. A., Straneo, F., Våge, K., and Årthun, M.: Nordic Seas heat loss, Atlantic inflow, and Arctic sea ice cover over the last century. Rev Geophys., 60, e2020RG000725, 2022

Smith, K. E., Burrows, M. T., Hobday, A. J., Sen Gupta, A., Moore, P. J., Thomsen, M., et al.: Socioeconomic impacts of marine heatwaves: Global issues and opportunities. Science, 374(6566), eabj3593. https://doi.org/10.1126/science.abj3593, 2021

WMO 2007: The Role of Climatological Normals in a Changing Climate (WMO/TD-No. 1377). Geneva.

WMO 2015: Seventeenth World Meteorological Congress (WMO-No. 1157). Geneva.

Xie, J. P., Counillon, F., Bertino, L., Tian-Kunze, X., and Kaleschke, L.: Benefits of assimilating thin sea ice thickness from SMOS into the TOPAZ system. Cryosphere, 10(6), 2745-2761, 2016

Xie, J. P., Raj, R. P., Bertino, L., Samuelsen, A., and Wakamatsu, T.: Evaluation of Arctic Ocean surface salinities from the Soil Moisture and Ocean Salinity (SMOS) mission against a regional reanalysis and in situ data. Ocean Sci., 15(5), 1191-1206, 2019

Xie, J. P., and Bertino, L.: EU Copernicus Marine Service Quality Information Document for the Arctic Ocean Physics Reanalysis Product, ARCTIC_MULTIYEAR_PHY_002_003, Issue 1.2, Mercator Ocean International, https://catalogue.marine.copernicus.eu/documents/QUID/CMEMS-ARC-QUID-002-003.pdf, last access: 20 June 2023, 2022

Xie, J. P., Raj, R. P., Bertino, L., Martinez, J., Gabarro, C., and Catany, R.: Assimilation of sea surface salinities from SMOS in an Arctic coupled ocean and sea ice reanalysis. Ocean Sci., 19(2), 269-287, 2023

Yang, X.-Y., Yuan, X. and Ting, M.: Dynamical link between the Barents-Kara sea ice and the Arctic Oscillation. J. Clim., 29, 5103-5122. doi: 10.1175/JCLI-D-15-0669.1, 2016